JOURNAL OF PROPULSION AND POWER
Vol. 27, No. 1, January–February 2011

Rheological and Thermal Behavior of Gelled Hydrocarbon Fuels

R. Arnold,* P. H. S. Santos,† O. H. Campanella,‡ and W. E. Anderson§
Purdue University, West Lafayette, Indiana 47907

DOI: 10.2514/1.48936

Rocket propulsion systems are bound to energetic propellant combinations to provide the best performance in conjunction with smallest possible storage volume. The application of a gelled fuel and a gelled oxidizer potentially combines the advantages of conventional solid and liquid propellants without some specific disadvantages of both individual systems. Gelled JP-8 and RP-1 fuels have been used to study the rheological behavior of gelled hydrocarbons. For all investigations fumed silica was used as a gelling agent with 4 to 7 wt%. Alongside a description of the gel mixing process, the paper discusses viscosity, stability, thixotropic behavior, and the viscoelastic properties of the gels through their storage and loss moduli as a function of gelling-agent amount. An extended Herschel–Bulkley model was applied to describe the viscosity characteristics of the hydrocarbon gels. Differential scanning calorimetry measurements showed only a slight influence of the gelling-agent amount on the heat of vaporization of the gels. The ungelled hydrocarbons featured a higher heat of vaporization than the gels.

Nomenclature

a	=	exponent
a_c	=	centripetal acceleration, m/s^2
c_p	=	specific heat capacity for constant pressure, J/(kg K)
d	=	distance, m
G'	=	storage modulus, N/m^2
G''	=	loss modulus, N/m^2
K	=	consistency index, Pa · s^n
M	=	gelling-agent mass fraction
m	=	mass, kg
n	=	power-law index
n_r	=	revolution speed, s^{-1}
Q	=	heat flow, W
R	=	cone radius, m
R^2	=	square of the multiple correlation coefficient
r	=	radius, m
T	=	temperature, K
T'	=	heating rate, K/ min
T_r	=	torque, Nm
t	=	time, s
ΔH_{vap}	=	heat of vaporization, kJ/kg
δ	=	phase angle, deg
γ	=	strain
$\dot{\gamma}$	=	shear rate, s^{-1}
η	=	dynamic viscosity, kg/(ms)
η_0	=	dynamic viscosity at low shear rate, kg/(ms)
η_∞	=	dynamic viscosity at infinite shear rate, kg/(ms)
ν	=	kinematic viscosity, m^2/s
ξ	=	torsion angle, deg
Θ_0	=	cone angle, deg
ρ	=	density, kg/m^3
σ	=	shear stress, N/m^2
σ_0	=	yield stress, N/m^2
ω	=	period of strain oscillation, s^{-1}

Subscripts

gel	=	gelling agent
ini	=	initial
liq	=	liquid
max	=	maximum
min	=	minimum
rem	=	remaining
sep	=	separated
tot	=	total
1, 2	=	counter

Received 14 January 2010; revision received 13 August 2010; accepted for publication 6 September 2010.

*Postdoctoral Scientist, Department of Aeronautics and Astronautics, Maurice J. Zucrow Laboratories, 500 Allison Road; arnold17@purdue.edu. Member AIAA.

†Graduate Research Assistant, Department of Agricultural and Biological Engineering, 225 South University Street; psantos@purdue.edu.

‡Professor, Department of Agricultural and Biological Engineering, 225 South University Street; campa@purdue.edu.

§Associate Professor, Department of Aeronautics and Astronautics, 701 West Stadium Avenue; wanderso@purdue.edu. Senior Member AIAA.

I. Introduction

THE advantages of gelled propellants compared to typical liquid and solid rocket propellants are liquid-propellant-like high performance, wide-range thrust control and reignitability, and solid-propellant-like storage behavior and safety aspects. Gels also provide the potential to add insoluble metallic particles such as aluminum, magnesium, or boron during the gel mixing process, with minimum particle-settling to increase energy density of the propellant and engine thrust [1,2]. Theoretical studies have shown that a replacement of the solid rocket boosters of the Space Transportation System with a propellant combination of O_2 and gelled RP-1/Al (55 wt% Al) could improve the payload of the space shuttle by up to 10% without changing the booster size, due to the increased energy density of the gelled propellants [3]. In addition, the specific impulse of a gelled RP-1 propellant combination will be lower than for pure O_2/RP-1. The payload increase of the gelled propellant results from a higher propellant mass, due to the increased energy density of the gelled propellants.

Gels can be stored like solids in the propellant tank, with a very good leakage behavior in terms of spillage and with a ruptured tank structure. When shear stress is applied to the shear-thinning gel, the viscosity is reduced. The gel now can be pumped with reasonable pressure loss requirements and injected into the combustion chamber almost like a typical liquid rocket propellant. For some gelling-agent types this process can be partially reversible with viscosity increase once the shear stress is removed from the gel [4,5].

To produce a gel, two different groups of gelling agents can be distinguished. Organic gelling agents such as hydroxypropylcellulose, hydroxyethylcellulose, and hydroxyalkylcellulose burn together with the fuel. Inorganic gelling agents such as silica (SiO_2), which is especially used to produce a nitric acid gel, remain unburned at the end of the combustion process.

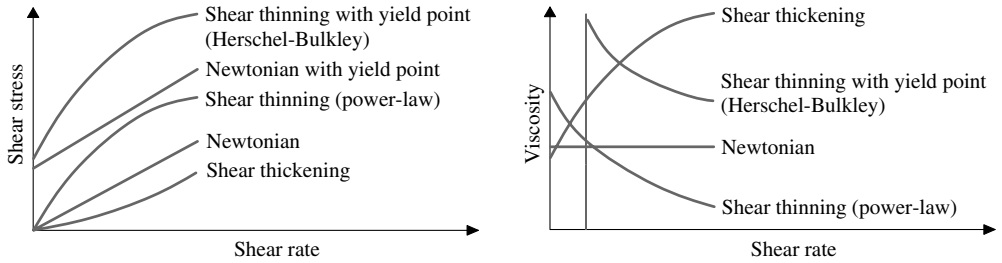

a) Shear stress vs. shear rate **b) Viscosity vs. shear rate**

Fig. 1 Shear stress and viscosity behavior for Newtonian and non-Newtonian fluids [44].

Investigations in the past concentrated on gelled hydrocarbon fuels such as JP-5, JP-8, JP-10 and RP-1, and also on gelled monopropellants such as MMH (monomethylhydrazine) and unsymmetrical dimethylhydrazine. A matter of particular interest is also the gelling of oxidizers such as white fuming nitric acid and IRFNA (inhibited red fuming nitric acid) [5–7]. Together with gelled MMH, these oxidizers can be used for the propulsion of hypergolic gelled rocket engines. With consideration of metallic powder addition, most promising gelled hypergolic propellant combinations for future rocket applications are MMH/Al/IRFNA and MMH/Al/NTO (nitrogen tetroxide). These propellant combinations could be used as a high-energy replacement of hypergolic MMH/NTO, which is used for example in the reignitable upper stage engine Aestus of the European Ariane 5 launcher. Gelled propellants are also of interest to missile applications. The first successful test fight of a missile system in 1999 using a carbon loaded MMH fuel gel and an IRFNA oxidizer gel demonstrated the technical readiness of the technology [8].

A gel consists at least the original propellant and the added gelling agent. The amount of gelling agent as well as the liquid/gelling-agent combination controls the rheological characteristics of the gel. Gels are non-Newtonian fluids which have an almost solidlike behavior when no shear stress is applied. Figure 1 depicts the behavior in terms of shear stress and viscosity as a function of shear rate for different Newtonian and non-Newtonian fluids. To provide both, a good storage behavior as well as a low pressure drop when pumping the propellant from the storage tank to the injector, gels envisaged for the application in rocket and airbreathing propulsion system have to show a shear-thinning behavior along with the presence of significant yield stress to conform a material classified as plastic (see Fig. 1a).

In general, for a Newtonian liquid the shear viscosity η is calculated independently of the shear rate $\dot{\gamma}$:

$$\eta = \frac{\sigma}{\dot{\gamma}} \tag{1}$$

Conversely, for a non-Newtonian liquid the viscosity η is dependent on the applied shear rate $\dot{\gamma}$. For the characterization non-Newtonian fluids without a yield point, the power-law model (Ostwald–de Waele model) is the most commonly used correlation [9]:

$$\eta = K\dot{\gamma}^{n-1} \tag{2}$$

where K is the consistency index, and n is the power-law index of the fluid. For $n = 1$ Eq. (2) describes a Newtonian fluid. However, for shear-thinning behavior the power-law index is $0 < n < 1$, and for shear-thickening (dilatant behavior) $n > 1$ (see Fig. 1 for different types of fluids).

The Herschel–Bulkley model (HB) is a simple description of the viscous behavior of nonlinear gels which considers a yield stress σ_0 for low and medium shear rates [9]:

$$\sigma = \sigma_0 + K\dot{\gamma}^n \tag{3}$$

Finally, an extended version of the Herschel–Bulkley equation (HBE) takes into account the minimum viscosity η_∞ at very high shear rates [9,10]:

$$\eta = \eta_0 + K\dot{\gamma}^{n-1} + \eta_\infty \tag{4}$$

Alongside the HBE, another model was provided from Carreau–Yasuda, which also considers viscosities at very low ($\to 0$) and very high ($\to \infty$) shear rates. However, this model neglects the existence of yield stress:

$$\eta = \eta_\infty + \frac{\eta_0 - \eta_\infty}{\{1 + (K\dot{\gamma})^a\}^{\frac{1-n}{a}}} \tag{5}$$

With the HBE or the Carreau–Yasuda models, viscosities at typical rocket engine and ramjet injection conditions with shear rates above $10^5\ s^{-1}$ can be considered, whereas the HB model would underpredict viscosities at these conditions, with values far below the viscosity of the pure liquid [11]. It is important to emphasize that neither of these models consider time-dependent effects.

Storage and loss moduli, $G'(\omega)$ and $G''(\omega)$, respectively, are parameters that describe a gel in terms of its viscoelastic characteristics, and in practical terms its strength and weakness. These moduli present the range of stored $G'(\omega)$ and dissipated $G''(\omega)$ energy fractions as a function of strain oscillation ω and the phase angle between shear rate and shear stress, as depicted in Fig. 2:

$$G'(\omega) = \frac{\sigma_0 \cos\delta}{\gamma_0} \tag{6}$$

$$G''(\omega) = \frac{\sigma_0 \sin\delta}{\gamma_0} \tag{7}$$

The phase angle between shear rate $\dot{\gamma}$ and shear stress σ characterizes the fluid, where $\delta = 90°$ describes a purely viscous liquid, and $\delta = 0°$ a purely elastic material. For $0° < \delta < 90°$ a viscoelastic fluid character can be observed. For a Newtonian liquid, G' becomes zero, whereas $G'' = 0$ for elastic solids. Viscoelastic materials can be characterized by $G' \neq 0$ and $G'' \neq 0$. Finally, the overall material function is given by [12]:

$$\frac{\sigma}{\gamma_0} = G'\sin(\omega t) + G''\cos(\omega t) \tag{8}$$

II. Materials and Measurement Technique

A. Fumed Silica as a Gelling Agent

For producing the gels, untreated fumed silica SiO_2 (CAB-O-SIL® grade M-5) was used. In general, silica results from a combustion process of silicon tetrachloride ($SiCl_4$) in a H_2/O_2 flame [see Eq. (9)]. Because of agglomeration, a fluffy white powder is created with an agglomeration size of less than 44×10^{-6} m and a

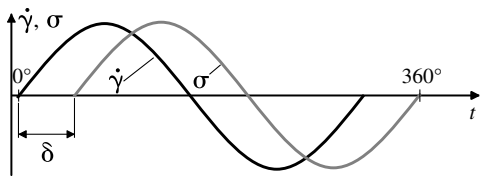

Fig. 2 Sinusoidal time variations of shear stress and shear rate.

Table 1 Properties of CAB-O-SIL M-5

B.E.T.[a] surface area, m^2/g	200
Tamped density, g/l	50
Specific gravity, g/cm^3	2.2
Average particle length, 10^{-6} m	0.2–0.3
Assay, % SiO_2	>99.8
Melting point, K	≈1983

[a]B.E.T. stands for an adsorption model for gases on a surface of a solid named after the physicists Brunauer, Emmett, and Teller.

hydrogen chloride level of less than 60 ppm after a following calcining process. The aggregate chains of the silica are hereby a composition of fused-together single particles [13]:

$$SiCl_4 + 2H_2 + O_2 \xrightarrow{2070\ K} SiO_2 + 4HCl \quad (9)$$

Table 1 gives an overview of typical properties of CAB-O-SIL M-5.[¶] The surface of the silica has hydrophilic characteristics and is capable of building up hydrogen bonds to create a gel when mixed with the liquid, due to chemical groups [isolated hydroxyl groups (hydrophilic), hydrogen-bonded hydroxyl groups (hydrophilic), and siloxane groups] that are attached to the surface of the silica during the formation process. The hydrogen bonds between single silica aggregates in a dispersed liquid system result in increased viscosity and rheological phenomenon named thixotropic behavior. The application of a shear force destroys the gel network between the aggregates and results in a reduced viscosity (see Fig. 3). The gel now can be injected and burned like conventional liquid propellants [14]. However, when the shear stress is removed from the system, hydrogen bonds can redevelop and increase the viscosity of the gel.

The quality of the network between the aggregates is thereby a function of the following main parameters [13]: 1) nature of the pure liquid, 2) nature and concentration of gelling agent, 3) degree of dispersion, 4) temperature of the system, and 5) degree of aging of the system.

In combination with non-hydrogen-bonding liquids such as aliphatic (no existence of aromatic rings, e.g., CH_4) and aromatic hydrocarbons and mineral oils, the single silica particles only can connect to each other, which results in a best possible network and also requires the lowest amount of silica (3–6% by total weight) to obtain desired rheological behavior. On the other hand, in combination with highly hydrogen-bonding systems such as acids, alcohols, and ketones, a much higher amount of silica is needed, due to undesirable bonds between the silica surface and the liquid system.

B. Hydrocarbon Fuels

Two different petroleum-derived hydrocarbon fuels were gelled with fumed silica for the present paper, rocket propellant RP-1 and jet propellant JP-8, both containing as many as 1000 compounds [15]. RP-1, per MIL-P-25576C [16] is a kerosene rocket propellant, which powers the first-stage boosters of the Delta and Atlas-Centaur rockets, and was also used in the first stage of the Saturn V moon rocket. Because of its high energy density in comparison with the high-energy liquid hydrogen, the propellant combination RP-1/liquid oxygen is also used in a great many of Russian booster engines (RD-170, RD-180) [17,18]. JP-8, per MIL-DTL-83133 [19] (jet propellant; NATO code F-34) is the U.S. Air Force primary jet fuel, replacing JP-4 in 1995 because of its less flammable character, better safety, and higher combat survivability. JP-8 is based on the civil fuel Jet-A1, but to provide high performance, additives for static dissipator, corrosion inhibitor, lubricity improver, and fuel-system icing inhibitor are added. Typical properties of the investigated hydrocarbon fuels JP-8 and RP-1 are summarized in Table 2 [19–24]. The same batches of JP-8 and RP-1 were used for all of the tests.

[¶]Data available online at http://www.freemansupply.com/MSDS/Combined/Fillers/Cabosil.pdf [retrieved 3 October 2010].

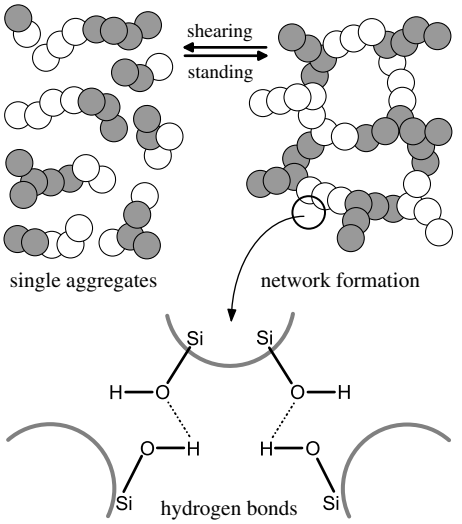

Fig. 3 Silica aggregates, hydrogen bonds, and network formation (according to [13]).

Since RP-1 is used as a cooling liquid in regeneratively cooled combustion chambers (e.g., RD-170, RD-180), a very low sulfur content is mandatory to prevent copper or copper alloy chamber walls from chemical damage due to copper corrosion by formation of Cu_2S [25,26]. For future applications, a further-developed rocket propellant RP-2 with only 0.1 mg/kg will be available to prevent coking at very high wall temperatures [27]. Coking or cracking at temperatures above approximately 650 K results in a detrimental thermal resistance of the propellant [28,29]. Furthermore, Cu_2S leads to damage in the chamber wall, increased overall pressure drop, and reduced cooling efficiency [30]. To provide high-temperature stability and also a good storage behavior, the amount of aromatics in the saturated hydrocarbon fuel RP-1 has been reduced in comparison to nonrocket hydrocarbon fuels such as JP-8 [31]. Because of the general lack of light hydrocarbons, RP-1 and JP-8 fuels have a relatively high flash point. It can be stated by now that the higher molecular weight of RP-1 will result in a higher gel stability and a higher initial viscosity.

C. Gel Mixing and Gel Stability

For the preparation of the gels, an acoustic high-shear-mixing technique (Resodyn Resonant-Acoustic® LabRAM) was used. The applied acoustic mixing process uses low-frequency, high-intensity acoustic energy, resulting in a uniform shear level inside the mixing container. For the mixing, the entire system oscillates in resonance frequency, which gives a very high dispersion in the mixing container. Microscale turbulence is created inside the medium by the acoustic waves, resulting in a very consistent mixing of the liquid and the gelling agent compared to conventional blade or impeller mixing for highly viscous or even solid materials in combination with a very short mixing time. Because of accelerations up to 100 g during the mixing process, very high shear rates are applied to the material [32].

Table 2 Fuel properties

	JP-8	RP-1
Approximate formula	$C_{11}H_{21}$	$C_{12}H_{23.4}$
Maximum aromatics, % by volume	25.0	5.0
Total maximum sulfur, % by mass	0.30	0.05
ρ at 288 K, g/cm^3	0.755–0.840	0.801–0.815
ν, 10^{-6} m^2/s	<8, at 253 K	1.96–2.24, at 293 K
Minimum flash point, K	311	316
Boiling point, K	430–573	420
Maximum freezing point, K	226	237
Minimum heat of combustion, MJ/kg	42.8	43.0

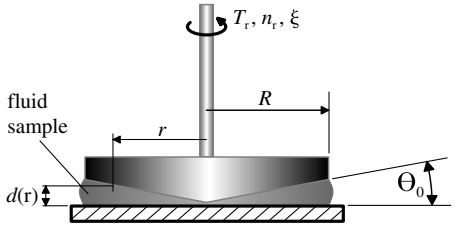

Fig. 4 Cone-and-plate rheometer configuration.

D. Propellant Characterization

For the detection of the rheological behavior of the gelled hydrocarbons JP-8 and RP-1, a rotational rheometer operated in controlled-rate mode was used. The rotational rheometer imposes strain to the liquid and measures the resulting stress for shear rates up to 1000 s^{-1}. The most common test geometries for a rotational rheometer are the parallel plate and the cone and plate. Whereas the parallel plate offers some advantages such as easy sample preparation, the cone-and-plate configuration has been used for the present investigations, because it allows a homogeneous strain distribution in the gelled liquid. Figure 4 depicts the cone-and-plate rheometer configuration as well as typical parameters such as cone angle Θ_0, cone radius R, torque T_r, torsion angle ξ, and shaft revolution speed n_r. Shear rate $\dot{\gamma}$ and viscosity η are functions of these geometric parameters [33]:

$$\dot{\gamma} = \frac{\mathrm{d}\gamma}{\mathrm{d}t} = \frac{r\mathrm{d}\xi}{\mathrm{d}t(r\tan\Theta_0)} = \frac{2\pi n_r}{\tan\Theta_0} \tag{10}$$

$$\eta = \frac{\sigma}{\dot{\gamma}} = \frac{3T_r\tan\Theta_0}{4\pi^2 n_r R^3} \tag{11}$$

For the present investigations, a cone angle $\Theta_0 = 2°$ and a cone radius $R = 20$ mm were used. A temperature-control system inside the equipment ensured a constant fluid temperature of 298 K during all rheological measurements.

By the use of a differential scanning calorimeter (DSC) combined with a thermogravimetric analysis (TGA), the influence of the gelling-agent amount on the latent heat of vaporization and further parameters such as the specific heat were investigated [34]. By comparison of the heat required to evaporate a small amount of the gelled propellant and a thermodynamically well-defined reference sample, the heat of vaporization can be detected by the DSC with a very high accuracy for the different gels as a function of the added gelling agent amount. The TGA determines the weight change due to vaporization of the sample as a function of the applied temperature with a very high precision.

III. Results and Discussion

To characterize the amount of silica in the gels, the mass fraction M describes the gelling-agent amount m_{gel} in comparison to the total propellant mass, given by the mixture of liquid m_{liq} and gelling agent m_{gel}:

$$M = \frac{m_{\mathrm{gel}}}{m_{\mathrm{liq}} + m_{\mathrm{gel}}} \tag{12}$$

Investigations have shown that a higher mixing time does not produce a higher viscosity of the mixed gel; rather, a shorter mixing time seems to improve the quality of the gel in terms of viscosity [35]. Especially for low shear rates, a significant decrease in viscosity has been observed for mixing times exceeding 80 s. Because of very high accelerations during the mixing process, the loss in viscosity for higher mixing times can be caused by interactions of the liquid with the hydrogen bonds of the silica particles [13], which affect and weaken the hydrogen bonds between the silica particles (see Fig. 3). The high shear mixing also increases the temperature of the mixed liquid, due to the very high accelerations in the range of 100–105 g, as depicted in Fig. 5 for a JP-8 gel with 5% silica. However, due to a negligible heating of only a few degrees Kelvin even for mixing times up to a few hundred seconds, the temperature influence on the viscosity for increasing mixing times can generally be discounted.

Based on the viscosity results, a mixing time of 60 s and mixing accelerations of approximately 100 g have been chosen to assure a preferable and reproducible gel quality within the present study.

Since propellants, especially in missile applications, are subjected to very high accelerations and vibrations during takeoff and flight, investigations have be done to make sure that the gels show no separation [6]. Centrifuge tests have been conducted that applied two constant accelerations ($a_c = 90$ and 1500 g) for a time period of 600 s, as depicted in Fig. 6. The separated liquid mass m_{sep} due to the acceleration has been compared with the initial propellant mass m_{tot} to describe the stability of the investigated gels:

$$m_{\mathrm{rem}} = m_{\mathrm{tot}} - m_{\mathrm{sep}} \tag{13}$$

The 6 and 7% gels show a quite stable behavior for accelerations $a_{\mathrm{c}} = 90$ g, whereas for higher accelerations only 70–80% remaining mass m_{rem} have been measured. A silica amount $M < 6\%$ did not show adequate stability, even for a lower acceleration. However, the RP-1 gel showed a more stable character than the JP-8 gel within the investigated range of added gelling agent and applied centripetal accelerations. These results are consistent with the investigated gel viscosity in Sec. III.A, where the rheological measurements have shown a higher viscosity for the RP-1 as well as the RP-1 gels in comparison to JP-8 and JP-8 gels.

A. Viscosity and Yield Stress

Figure 7 depicts the viscosity η as a function of shear rate $\dot{\gamma}$ and silica amount M for JP-8 and RP-1. A significant increase of the

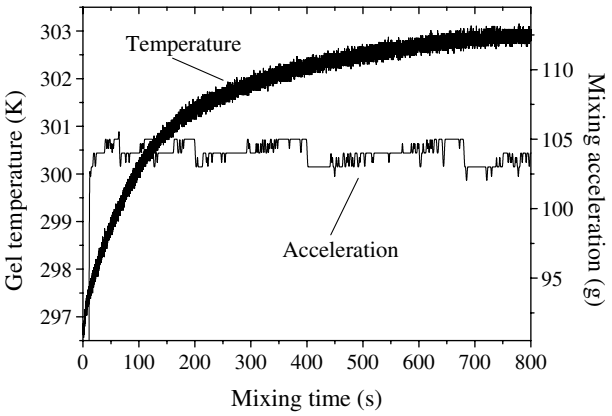

Fig. 5 Gel temperature during mixing (JP-8, $M = 5\%$).

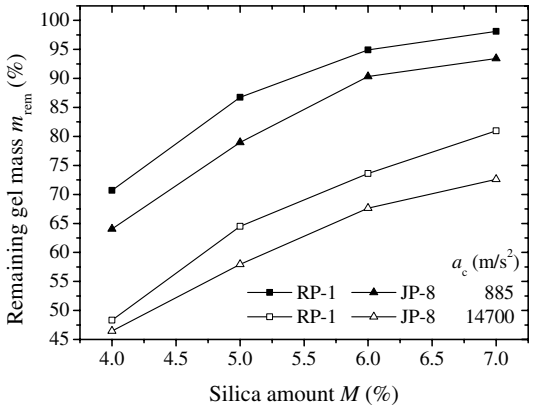

Fig. 6 Gel stability.

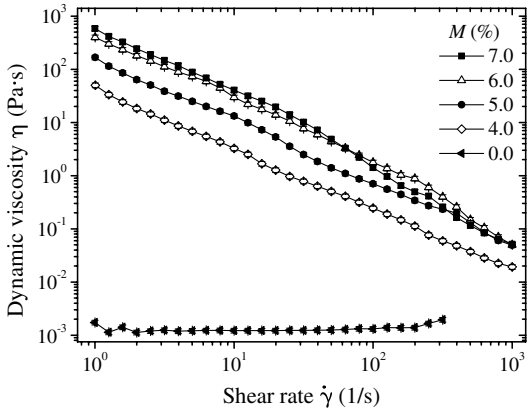

a) JP-8

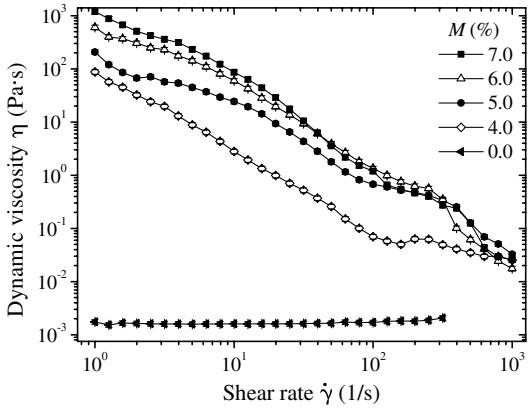

b) RP-1

Fig. 7 Viscosity as function of silica amount.

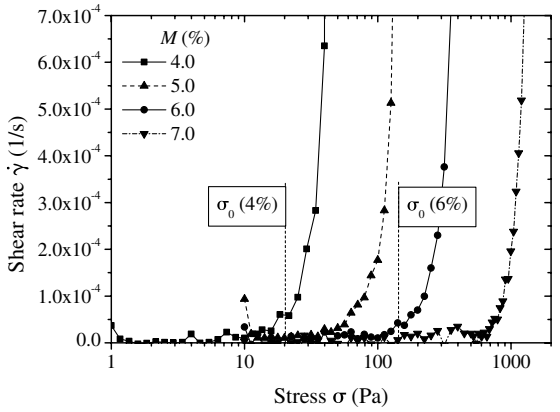

a) JP-8

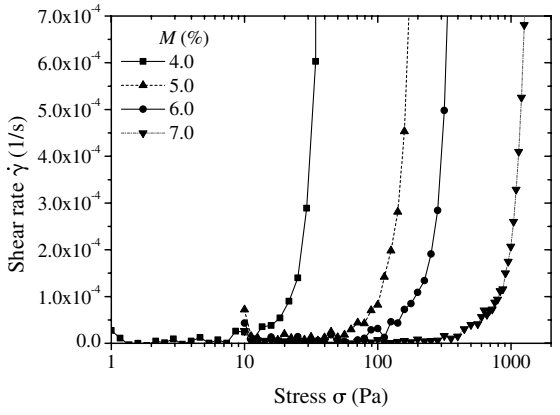

b) RP-1

Fig. 9 Yield stress.

viscosity for both hydrocarbon fuels can be stated with an increasing gelling-agent amount in comparison to the ungelled liquids. Viscosities of the pure liquids are 1.32 mPa · s (JP-8) and 1.68 mPa · s (RP-1) and agree very well with data from literature (RP-1: 1.6 mPa · s at 298 K [36]). For the gels, the influence of the fumed silica is not only visible for low shear rates, but remains noticeable with a reduced significance up to higher shear rates. The differences between the Newtonian-like pure liquids RP-1 and JP-8, where the viscosity is not a function of the applied shear rate, and the non-Newtonian behavior of the gelled hydrocarbons is clearly visible in Fig. 7.

For both the pure and the gelled RP-1 a higher viscosity has been measured in the low shear range up to approximately 100 s^{-1}, as a comparison of the RP-1 and JP-8 viscosities points up in Fig. 8. The viscosity of the pure RP-1 is about 1.3 times higher than the viscosity of the pure JP-8, independent of the applied shear rate. However, when adding a gelling agent, the viscosity ratio of the gels, η_{RP-1}/η_{JP-8}, increases up to approximately 2.6 for low- and medium-range shear rates for a gelling-agent amount $M = 7\%$ and up 1.8 for $M = 5\%$. However, for higher shear rates of greater than 100 s^{-1}, an equalization of the viscosities of the different gels can be seen. The higher amount of carbon atoms in the RP-1 molecular structure (see Table 2) is responsible for the higher viscosity and for the higher stability (see Fig. 6).

The yield stress σ_0 defines the amount of stress that non-Newtonian material can bear without showing flow. When applying more stress than the yield stress, a permanent deformation of the material will be occur. For a liquid, the yield stress describes the minimum stress that must be applied to make the fluid flow. Figure 9

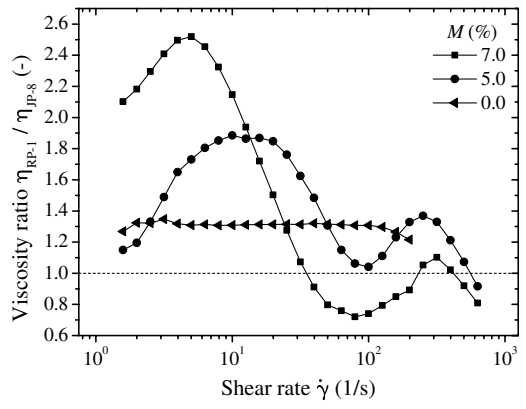

Fig. 8 Viscosity ratio.

Table 3 HBE parameters for gelled JP-8

M, %	4.0	5.0	6.0	7.0
σ_0, Pa	22	58	160	550
K, Pa · s^n	27.13	103.7	234.8	371.9
n	−0.85	−0.45	−0.18	−0.33
η_∞, mPa · s	1.32	1.32	1.32	1.32
R^2	0.997	0.996	0.999	0.998

Table 4 HBE parameters for gelled RP-1

M, %	4.0	5.0	6.0	7.0
σ_0, Pa	18	55	140	460
K, Pa · s^n	67.64	73.27	427.3	638.8
n	−0.56	−0.14	−0.08	−0.18
η_∞, mPa · s	1.68	1.68	1.68	1.68
R^2	0.997	0.955	0.987	0.996

depicts the applied stress σ as a function of the shear rate $\dot{\gamma}$ for the JP-8 and RP-1 gels, featuring a silica content of $M = 4$–7%. The influence of the gelling-agent amount M on the yield stress is also clearly visible, since more gelling agent results in a significantly higher yield stress of the gels. The yield stress data for the different gels are summarized in Tables 3 and 4 (Sec. III.C) for JP-8 and RP-1 gels, respectively.

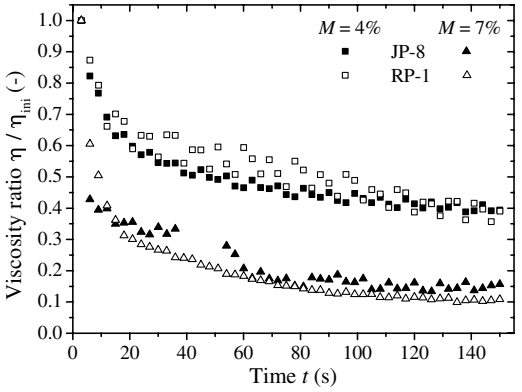

Fig. 10 Viscosity as a function of time ($\dot{\gamma} = 100$ 1/s).

B. Thixotropic Behavior

Shear-thinning non-Newtonian fluids show a decreasing viscosity when an increasing shear rate is applied. Thixotropic fluids also show a decreasing viscosity over time when a constant shear rate is maintained.

Figure 10 depicts the time dependency of the investigated hydrocarbon gels, applying a constant shear rate $\dot{\gamma} = 100$ 1/s. The initial viscosity η_{ini} is significantly reduced within the first 20 s of shearing: about 40% for the 4% gels and about 70% for the 7% gels. Further shearing reduces the viscosity more. JP-8 and RP-1 gels with the same amount of gelling agent behave comparably; however, the influence of the gelling-agent amount M is clearly visible. The viscosity reduction for gels with a higher silica amount is more pronounced than the time-dependent viscosity decrease of gels with a lower amount of gelling agent. Finally, the viscosity can be written as

$$\eta = \eta(\dot{\gamma}, M, t) \tag{14}$$

Because of the application of shear to the silica gels, the interaggregate hydrogen bonds break, which leads to a decrease of

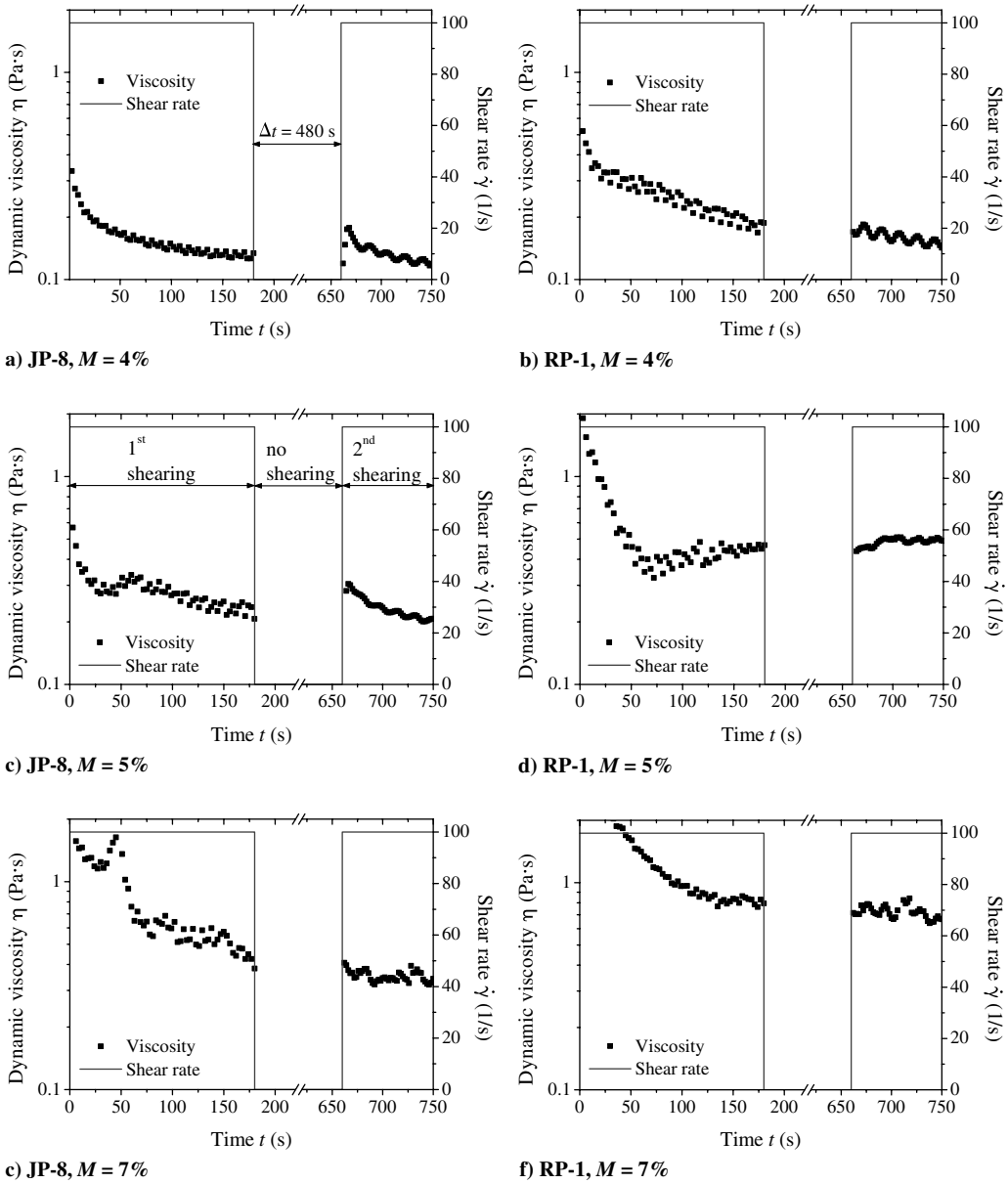

a) JP-8, $M = 4\%$ **b) RP-1, $M = 4\%$**

c) JP-8, $M = 5\%$ **d) RP-1, $M = 5\%$**

c) JP-8, $M = 7\%$ **f) RP-1, $M = 7\%$**

Fig. 11 Thixotropic behavior.

the apparent gel viscosity. It has been reported that once the shear force has been removed, the bonds rebuild over time and the viscosity approaches its original value [13]. This behavior may be restrictive for the application in a gelled-propellant engine, since the redevelopment of the hydrogen bonds would increase viscosity and pressure loss of the entire system. Once pumped from the storage tank, gelled propellants should show a low viscosity to unburden the pump system and good vaporization and combustion behavior. Figure 11 depicts the application of a shear rate $\dot{\gamma} = 100\ 1/\mathrm{s}$ for 180 s to destroy the hydrogen bond system and to break the gel. After a time interval of $\Delta t = 480$ s with no shearing, the original shear rate is applied again. It is clearly visible that there is no gel recovery after this time. The gel viscosity after the break is comparable to the viscosity when the shearing is stopped. This behavior is independent of the gelling-agent amount for the RP-1 and JP-8 gels. Since the gel structure is destroyed mostly after the first shearing period within the present investigations, the viscosity is only slightly reduced in the second shearing period. This can also be seen in Fig. 10, with a flattening of the viscosity slope for higher shearing times $t > 100$–120 s. However, the gel structure is not always destroyed in all propulsion applications.

C. Gel Modeling

Based on the yield stress results from the previous section, an extended Herschel–Bulkley model (see Sec. I) was used to characterize the gels investigated for the present study. By the use of Eq. (4), shear stress σ and viscosity η as a function of the shear rate $\dot{\gamma}$ for the HBE model can be written as [10]

$$\sigma(\dot{\gamma}) = \sigma_0 + K\dot{\gamma}^n + \eta_\infty \dot{\gamma} \qquad \eta(\dot{\gamma}) = \frac{\sigma_0}{\dot{\gamma}} + K\dot{\gamma}^{n-1} + \eta_\infty \tag{15}$$

Tables 3 and 4 give an overview of the Herschel–Bulkley parameters σ_0, K, n, and η_∞. For the gel viscosity at very high shear rates $\dot{\gamma} \to \infty$, the simplifying assumption of an agreement with the viscosity of the pure ungelled liquids RP-1 and JP-8, respectively, has been done:

$$\eta_\infty \approx \eta_{\mathrm{RP-1;\,JP-8}} \tag{16}$$

By definition, a power-law index $0 < n < 1$ describes the behavior of a shear-thinning fluid [12,33]. In a $\log(\dot{\gamma}) - \log(\eta)$ diagram, however, the exponent n characterizes the slope of the extended Herschel–Bulkley line, as depicted in Fig. 12 using the example of a $M = 4\%$ JP-8 gel. The slopes for $n = 0$ and 1 divide the typical regions of shear-thinning, Newtonian ($n = 1$), and shear-thickening behavior ($n > 1$). Because of the highly shear-thinning and thixotropic characteristics of the investigated hydrocarbon gels, the rheological measurements show a power-law index $n < 0$ (see Fig. 12), since the slope of the HBE-fitting line is slightly steeper than for the classical shear-thinning region given by $n > 0$.

The negative power-law indices of the hydrocarbon gels can be explained by simplifications and restrictions of the gel modeling. Common models such as the power-law model or the HBE only describe the effect of the shear rate on the gel viscosity, while ignoring the effect of time. However, the gels are not time-independent. Time-independent shear-thinning models only consider how the viscosity changes for an applied shear rate, regardless of the time. If the shear rate for a shear-thinning fluid is increased, a decrease in viscosity will be observed. If the fluid is also time-dependent, the actual viscosity will not be maintained if a constant shear rate is applied to the material. On the other hand, a shear-thinning time-dependent fluid will show not only a decrease of viscosity due to increased shear rate, but also a decrease of viscosity due to a breakdown of the gel structure. This superposition leads to a drastic decrease of viscosity in conjunction with the obtained negative values of the power-law index n (see Tables 3 and 4). The time-dependent breakdown of the gel structure can also be observed in Fig. 11. For a constant shear rate, the viscosity of the JP-8 and RP-1 gels decreases significantly, independently of the amount of gelling agent.

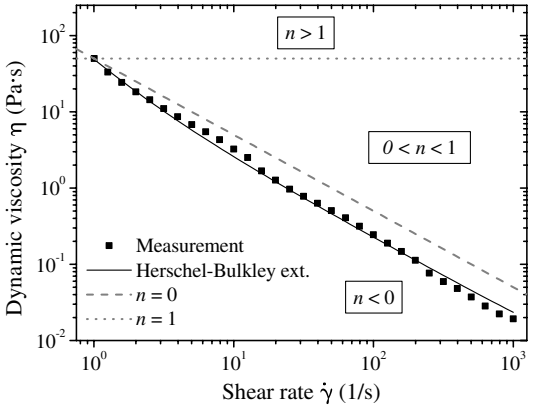

Fig. 12 Gel modeling (JP-8, $M = 4\%$).

D. Dynamic Rheological Properties

Figure 13 depicts the strain dependence of the storage moduli G' for JP-8 and RP-1 gels with 4 and 7% silica at a temperature of 298 K and an applied frequency of 5 Hz. For all investigated gel samples, the storage modulus remained constant at low-amplitude deformations and decreased after a critical deformation value with increasing deformation. This range in which the fluid is independent of the strain characterizes its linear viscoelastic region. The critical deformation values were around 2–3% for JP-8 gels and 3–4% for RP-1 gels. Neither the fluid nor the silica concentration has a significant influence on the critical deformation in which the dependency shows up. However, the magnitude of storage modulus

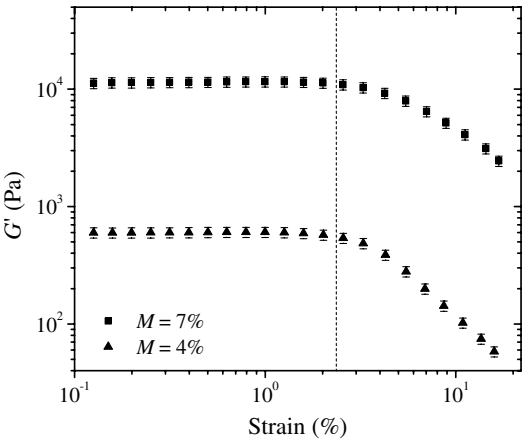

a) JP-8

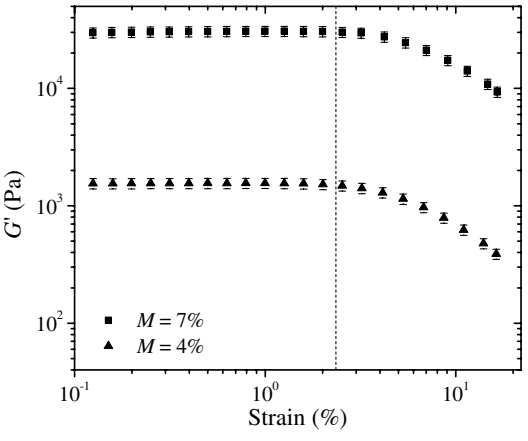

b) RP-1

Fig. 13 G' as a function of strain.

G' increases when the silica amount M is increased. The strength of the gel can be characterized by its storage modulus measured in the linear viscoelastic regime, and the effect of gellant concentration can be analyzed.

Figure 14 shows the positive effect of the silica concentration on the gel strength and the power-law dependence on the gellant concentration. This dependence can be characterized with $G' \propto M^{5.30}$ and $G' \propto M^{5.56}$ for JP-8 and RP-1 gels, respectively. At same silica concentrations M, the strength of RP-1 gels is at least twice as high as the JP-8 gel strength, but the influence of the silica concentration on both gels is comparable, since the power-law exponents are of the same order. The higher strength of the RP-1 gels comes along with a higher viscosity, as documented in Sec. III.A. Figure 14 also depicts the effect of the silica concentration on the yield stress σ_0, which can be characterized with $\sigma_0 \propto M^{6.4}$ and $\sigma_0 \propto M^{6.3}$ for JP-8 and RP-1 gels, respectively. Thus, measured gel properties G' and σ_0 can be described over almost three orders of magnitude within a wide range of gelling-agent concentrations. Previous investigations with silica nanocomposite ion gels have found similar dependencies with $G' \propto M^{4.65}$ and $\sigma_0 \propto M^{4.53}$ [37]. For potassium hydroxide solutions with silica and potassium chloride, similar results have been obtained with $G' \propto M^{4.2}$ [38].

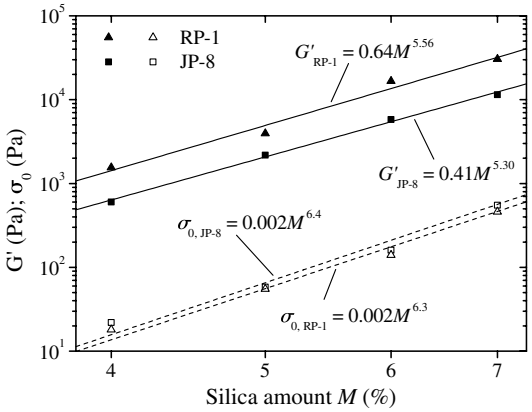

Fig. 14 Gel strength dependence on silica concentration.

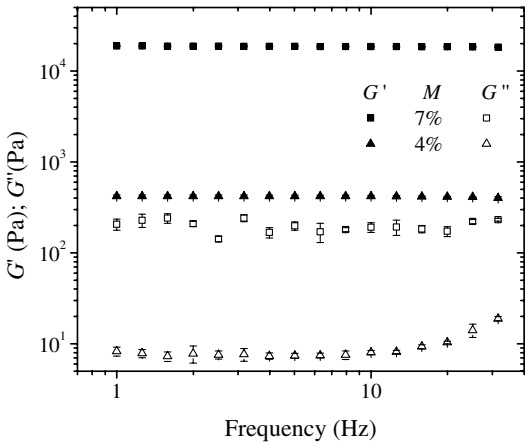

a) JP-8

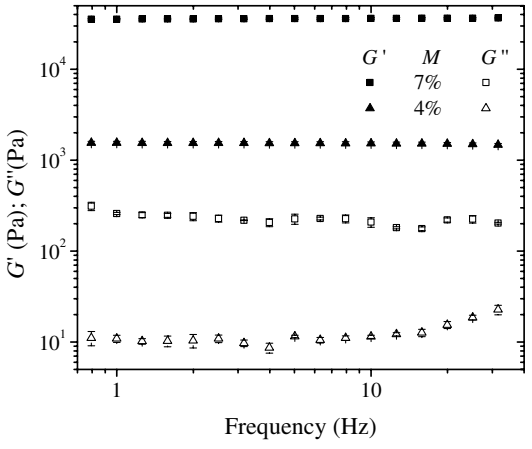

b) RP-1

Fig. 15 G' and G'' as a function of frequency (1% strain).

Frequency-sweep tests have been carried out to investigate the frequency dependence of storage and loss moduli G' and G'', respectively. For a gel, the storage modulus G' has to be some orders of magnitude higher than the loss modulus G'', since the applied force results in a largely elastic deformation of the gel structure. Figure 15 depicts that both storage and loss moduli are independent of frequency over the entire investigated range of 0.5–40 Hz, indicating the elastic nature of these gels. All measurements have been performed in the linear viscoelastic region (see Fig. 13), applying 1% strain at a temperature 298 K. In addition, the measurements show that the storage moduli are significantly higher than the loss moduli for all silica concentrations, so all gel samples exhibit a typical solidlike behavior of the gel structure. Similar to the storage moduli, the loss moduli G'' of the hydrocarbon gels are increased significantly with a higher gelling-agent concentration. The effectiveness of the added silica on the gel quality can be seen in Fig. 15 by an increase of the storage moduli of almost two orders of magnitude within the range of 4–7% gelling-agent amount for the JP-8 and RP-1 gels. The loss moduli of the investigated gels show a comparable behavior.

E. Thermal Characterization

The latent heat of vaporization ΔH_{vap} (also enthalpy of vaporization) is the required amount of energy to transform a given amount of a fluid from the liquid to the gaseous phase without changing the temperature of the substance. It is an important parameter for combustion systems where a liquid–vapor phase change antedates the combustion process [39]. For droplet burning, the burning velocity can be related to the Spalding transfer number, which represents the enthalpy ratio exiting the gas and entering the droplet during phase-transformation processes [40]. Since the heat of vaporization is proportional to the reciprocal of the Spalding number, and a lower Spalding number results in a slower burning behavior, a knowledge of the influence of the additional gelling-agent amount on the heat of vaporization is mandatory. For hydrocarbon JP-5 and an organic gelling agent, previous investigations have shown that the latent heat of vaporization can increase by almost 60% for a gel containing 5% gelling agent [41].

To determine the temperature range in which the evaporation occurs, TGA was conducted, as depicted in Fig. 16 for pure and gelled JP-8. The mass-fraction ratio between actual sample mass m and initial sample mass m_0 is plotted as a function of applied

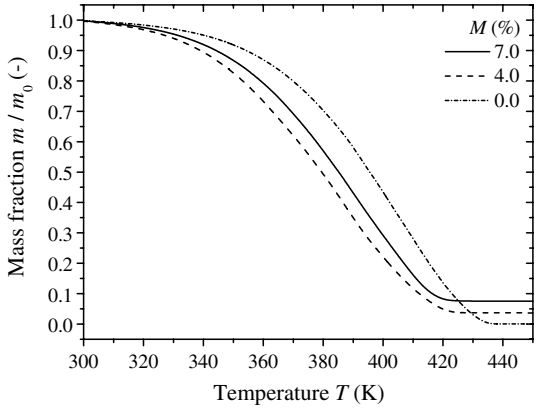

Fig. 16 TGA for JP-8.

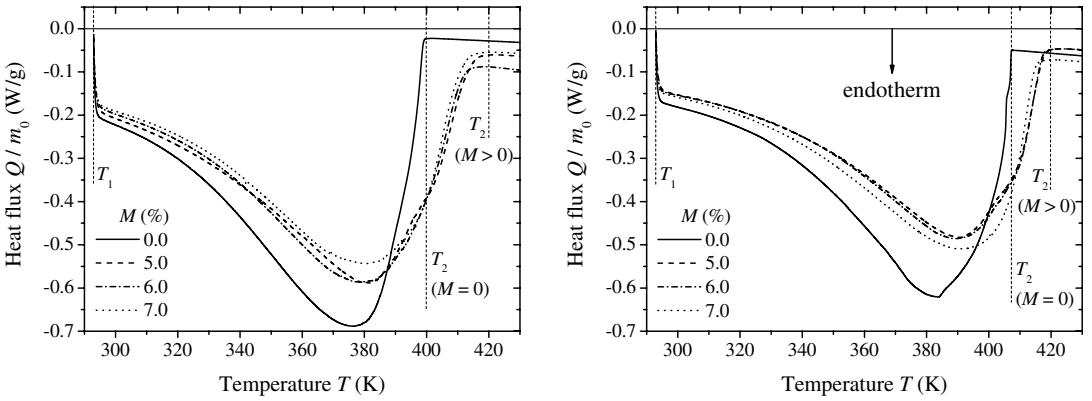

a) JP-8 **b) RP-1**

Fig. 17 Differential scanning calorimeter measurements.

temperature. The temperatures for both pure and gelled liquids can be estimated in the range of approximately $T = 300$–420 K. JP-8 and RP-1 gels show comparable temperature ranges.

Figure 17 depicts thermograms for vaporization for JP-8 and RP-1 as a function of gelling-agent amount. A heating rate of $T' = 20$ K/ min was applied for all tests. Vaporization for pure and gelled hydrocarbons starts immediately at a comparably low temperature of about $T_1 = 295$ K. The vaporization rate increases with increasing temperature. After the heat release peak, the vaporization is finished. Characteristics of the gelled and ungelled hydrocarbon measurements are similar to DSC investigations using benzene [42] and isopropylnitrate [43].

For the ungelled hydrocarbons, the endothermic peak is reached at approximately 375 and 385 K for JP-8 and RP-1, respectively. Vaporization is completed at about $T_2 = 400$ and 405 K for JP-8 and RP-1, respectively. The endothermic heat release peak due to the liquid–gaseous phase transition is more pronounced for JP-8 with a heat flux of almost -0.7 W/g.

Pure and gelled fuels show a similar vaporization behavior at low temperatures. At higher temperatures, a more significant flux has been measured for the gelled liquids. The endothermic heat flux peak is also higher for both types of gels, with approximately -0.6 and -0.5 W/g for JP-8 and RP-1 gels, respectively. The temperature of the minimum heat flux is higher than that of the ungelled liquids. Vaporization is completed at approximately $T_2 = 420$ K for JP-8 and RP-1 gels. For both gelled liquids, the gelling-agent amount seems to be insignificant for the vaporization behavior, as shown in Fig. 17 for $M = 5$–7%. The higher temperature of the endothermic peak for gels indicates that the escape of the liquid particles to the vapor phase is restricted by the gel network.

The enthalpy of vaporization ΔH_{vap} can be calculated by analyzing the area of the endothermic event in Fig. 17, given by $t_1(T_1)$ and $t_2(T_2)$. A larger endothermic area indicates more necessary energy to vaporize the material:

$$\Delta H_{\text{vap}} = \int_{t_1}^{t_2} \mathrm{d}Q\,\mathrm{d}t = \frac{1}{T'}\int_{T_1}^{T_2} \mathrm{d}Q\,\mathrm{d}T \tag{17}$$

Table 5 Heat of vaporization

M, %	0.0	4.0	5.0	6.0	7.0
$\Delta H_{\text{vap,JP-8}}$, kJ/kg	413.3	383.8	361.3	346.4	340.5
$\Delta H_{\text{vap,RP-1}}$, kJ/kg	358.5	322.7	304.6	302.6	299.2

Table 6 Heat of vaporization, normalized

M, %	0.0	4.0	5.0	6.0	7.0
$\Delta H_{\text{vap,JP-8}}$, kJ/kg$_{\text{fuel}}$	413.3	399.2	379.4	367.2	364.3
$\Delta H_{\text{vap,RP-1}}$, kJ/kg$_{\text{fuel}}$	358.5	335.6	319.8	317.7	320.1

Table 5 summarizes the enthalpy of vaporization as a function of gelling-agent amount for the investigated liquids. The addition of the gelling agent results in a reduced endothermic heat flux, but an expanded temperature range, compared to the heat flux behavior of the ungelled JP-8 and RP-1, as depicted in Fig. 17.

The heat of vaporization results for pure JP-8 and RP-1 are in good agreement with data from literature with $\Delta H_{\text{vap}} = 428$ kJ/kg for JP-8 and $\Delta H_{\text{vap}} = 308$ kJ/kg for RP-1 [24].

For gels, a reduced heat of vaporization was measured. The presence of silica seems to push the hydrocarbon molecules to a more free state with a reduced hydrocarbon density inside the gel which requires less energy to vaporize. The loose coupling of the hydrocarbons and the silica structure within the gel also indicates a reduced heat of vaporization in comparison to the ungelled liquids. Since the measurements of the DSC consider the heat flux per mass, the amount of evaporable liquid is also reduced with an increasing gelling-agent amount, which reduces the effective heat of vaporization. Table 6 summarizes the normalized heat of vaporization measurements based on the amount of propellant mass of the gels m_{fuel} instead of the total gel mass m_{tot} containing noncombustible inorganic silica particles and fuel. The heat of vaporization of the gels is still reduced compared to the heat of vaporization of the pure hydrocarbons; however, the influence of the gelling-agent amount is much less significant when the propellant mass instead of the gel mass is used as the basis (see Tables 5 and 6).

Finally, a reduced heat of vaporization of the gels may be explained to some extent by the fact that gels behave differently from the pure liquid, and the heat of vaporization describes only the phase change from liquid to gaseous. However, previous investigations using JP-5 with an organic gelling agent have shown an increase of the heat of vaporization of approximately 80% in the range between 0 and 5% of added gelling agent [41]. This can be explained by a much stronger connection of the propellant molecules and the organic gelling agent within the gel structure, which is also reflected in the much higher gel stability of organic gels.

F. Error Analysis

The error of the gelling-agent mass fraction can be estimated with $\Delta M < 0.1\%$. All rheological measurements have been performed three times. The standard deviation of the mean value has been calculated for all measurements, featuring a 95%-confidence interval. For rheological measurements, the absolute accuracy of the rotational rheometer is not dominant, but other parameters are dominant, such as the gel stiffness, vaporization of the liquid during the measurements, and the amount of gel used for the characterization. Depending on the applied shear rate, the measurement error of the viscosity can be specified with maximal $\Delta\eta = 8$–12% for shear rates up to 10 s^{-1} and $\Delta\eta = 5$–10% for shear rates higher than 10 s^{-1}. The errors for storage and loss moduli $\Delta G'$ and $\Delta G''$ have been found independently of the applied frequency within the range of 3–4%. For the yield stress, the error can be calculated with

Table 7 Summary conclusion chart for JP-8/silica and RP-1/silica gels

Aspect for increasing silica amount, $M \uparrow$	Tendency[a]	Remark
Gel stability	$\uparrow$	Significant silica amount necessary for stable gels; higher stability for RP-1/silica gels
Viscosity	$\uparrow$	Significant increase for increasing silica amount; higher values for RP-1/silica gels; gel structure breaks when shear is applied
Yield stress	$\uparrow$	Slightly higher yield stress for JP-8/silica gels
Thixotropicy	$\rightarrow$	No gel recovery after gel network is broken
Storage modulus	$\uparrow$	Linear viscoelastic region visible; independent of frequency over the investigated range
Loss modulus	$\uparrow$	Independent of frequency over the investigated range
Heat of vaporization	$\downarrow$	Higher values For JP-8/silica gels
Gel modeling	——	Extended Herschel–Bulkley with yield stress

[a]$\uparrow$ increases; $\downarrow$ decreases; $\rightarrow$ stays constant.

$\Delta\sigma_0 \approx 10$–$15\%$, since the sudden increase of the shear rate after passing the yield point is hard to detect for the stiff silica gels. TGA and DSC measurements have been done twice. The estimated error for the heat of vaporization is between 5–8%.

IV. Summary Chart

Because of the broad variety of experimental investigations with JP-8/silica and RP-1/silica gels, a summary conclusion chart is given with Table 7. Rheological and thermal behaviors of the investigated gelled hydrocarbon fuels are characterized by giving a tendency for increasing silica amount.

V. Conclusions

Within the present study, two gelled hydrocarbon fuels, JP-8 and RP-1, have been investigated experimentally. Fumed silica with concentrations of 4–7% has been used as an inorganic gelling agent. The amount of the added gelling agent showed significant influence on the viscosity of the gels for low as well as high shear rates. Even with small amounts of silica, the viscosity can be increased significantly. The gel stability is also a function of the gelling-agent amount, whereas only gels with a higher silica amount showed a satisfactorily stability during centrifuge tests. The investigation of the storage and loss moduli displayed the solidlike character of the unsheared gels. Since the gels feature a yield stress, an extended Herschel–Bulkley model has been applied to characterize the gels. Because of the high-shear-thinning behavior and the time dependency, comparable low power-law indices are necessary to describe the gels. Investigations regarding the heat of vaporization have shown a decrease of necessary energy to evaporate gels in comparison to ungelled JP-8 and RP-1 fuels.

Future investigations at Purdue University will not only include gelled hydrocarbon fuels, but will also consider the rheological behavior of rocket engine fuel monomethylhydrazine, using organic cellulose-based gelling agents such as hydroxypropylcellulose and hydroxyethylcellulose.

Acknowledgments

The research presented in this paper was made possible with the financial support of the U.S. Army Research Office under the Multi-University Research Initiative (MURI) grant number W911NF-08-1-0171. The support of M. A. Carignano is greatly acknowledged by the authors.

References

[1] Sutton, G. P., and Biblarz, O., *Rocket Propulsion Elements*, 7th ed., Wiley, New York, 2001.

[2] Teipel, U., and Forter-Barth, U., "Rheological Behavior of Nitromethane Gelled with Nanoparticles," *Journal of Propulsion and Power*, Vol. 21, No. 1, Jan.–Feb. 2005, pp. 40–43. doi:10.2514/1.3471

[3] Palaszewski, B., and Zakany, J. S., "Metallized Gelled Propellants: Oxygen/RP-1/Aluminium Rocket Combustion Experiments," 31st AIAA/ASME/SAE/ASEE Joint Propulsion Conference and Exhibit, San Diego, CA, AIAA Paper 1995-2435, July 1995.

[4] Natan, B., and Rahimi, S., "The Status of Gel Propellants in Year 2000," *Combustion of Energetic Materials*, edited by K. K. Kuo and L. deLuca, Begel House, Boca Raton, FL, 2001.

[5] Solomon, Y., Natan, B., and Cohen, Y., "Combustion of Gel Fuels Based on Organic Gellants," *Combustion and Flame*, Vol. 156, 2009, pp. 261–268. doi:10.1016/j.combustflame.2008.08.008

[6] Pein, R., "Gel Propellants and Gel Propulsion," *5th International High Energy Materials Conference and Exhibit DRDL*, Hyderabad, India, Nov. 2005.

[7] Birinci, E., Gevgilili, H., Kalyon, D., Greenberg, B., Fair, D., and Perich, A., "Rheological Characterization of Nitrocellulose Gels," *Journal of Energetic Materials*, Vol. 24, 2006, pp. 247–269. doi:10.1080/07370650600791262

[8] Hodge, K., Crofoot, T., and Nelson, S., "Gelled Propellants for Tactical Missile Applications," 35th AIAA/ASME/SAE/ASEE Joint Propulsion Conference & Exhibit, Los Angeles, AIAA Paper 99-2976, June 1999.

[9] Ferguson, J., and Kemblowski, Z., *Applied Fluid Rheology*, Elsevier, New York, 1991.

[10] Madlener, K., and Ciezki, H., "Analytical Description of the Flow Behavior of Extended Herschel–Bulkley Fluids with Regard to Gel Propellants," *36th International Annual Conference of ICT & 32nd International Pyrotechnics Seminar*, Karlsruhe, Germany, June 2005.

[11] Ciezki, H. K., and Natan, B., "An Overview of Investigations on Gel Fuels for Ramjet Applications," *17th International Symposium on Airbreathing Engines (ISABE 2005)*, Munich, Sept. 2005.

[12] Morrison, F. A., *Understanding Rheology*, Oxford Univ. Press, Oxford, 2001.

[13] "CAB-O-SIL® Untreated Fumed Silica–Properties and Functions, Mechanisms of CAB-O-SIL®," Cabot Corp., Rept. CGEN-8A, Boston, 2009.

[14] Mordosky, J. W., Zhang, B. Q., Kuo, K. K., Tepper, F., and Kaledin, L. A., "Spray Combustion of Gelled RP-1 Propellants Containing Nano-Sized Aluminium Particles in Rocket Engine Conditions," 37th AIAA/ASME/SAE/ASEE Joint Propulsion Conference and Exhibit, Salt Lake City, UT, AIAA Paper 2001-3274, July 2001.

[15] Mawid, M. A., Park, T. W., Sekar, B., and Arana, C., "Sensitivity of JP-8 Fuel Combustion and Ignition to Aromatic Components," 39th AIAA/ASME/SAE/ASEE Joint Propulsin Conference and Exhibit, Huntsville, AL, AIAA Paper 2003-4938, July 2003.

[16] "Propellant, Rocket Grade Kerosene," U.S. Dept. of Defense, MIL-P-25576C, 10 Feb. 1967.

[17] Sutton, G. P., "History of Liquid-Propellant Rocket Engines in Russia, Formerly the Soviet Union," *Journal of Propulsion and Power*, Vol. 19, No. 6, 2003, pp. 1008–1037. doi:10.2514/2.6943

[18] Sutton, G. P., "History of Liquid Propellant Rocket Engines in the United States," *Journal of Propulsion and Power*, Vol. 19, No. 6, 2003, pp. 978–1007. doi:10.2514/2.6942

[19] "Turbine Fuel, Aviation, Kerosene Type, JP-8 (NATO F-34), NATO F-35, and JP-8 + 100 (NATO F-37)," U.S. Dept. of Defense, MIL-DTL-83133F, 11 April 2008, .

[20] "Toxicological Profile for JP-5 and JP-8," U.S. Dept. of Health and Human Services, Agency for Toxic Substances and Disease Registry, Div. of Toxicology/Toxicology Information Branch, Atlanta, Aug. 1998, http://www.atsdr.cdc.gov/toxprofiles/tp121-p.pdf [retrieved 4 Oct. 2010].

[21] "Fuel, Diesel, Referee Grade," U.S. Dept. of Defense, MIL-DTL-46162E, 2 Nov. 2002.

[22] Malik, J. G., Graber, F. W., and Kelle, E. E., "Report of the Determination of Various Physical Properties of RP-1," General

Dynamics/Convair, Rept. MP 57-684, San Diego, CA, 11 Dec. 1958.
[23] "Handbook of Aviation Fuel Properties," Coordinating Research Council, Rept. 635, Alpharetta, GA, 2004.
[24] Chickos, J. S., and Zhao, H., "Measurement of the Vaporization Enthalpy of Complex Mixtures by Correlation-Gas Chromatography. The Vaporization Enthalpy of RP-1, JP-7, and JP-8 Rocket and Jet Fuels at $T = 298.15$ K," *Energy and Fuels*, Vol. 19, 2005, pp. 2064–2073.
[25] Rosenberg, S. D., and Gage, M. L., "Compatibility of Hydrocarbon Fuels with Booster Engine Combustion Chamber Liners," *Journal of Propulsion and Power*, Vol. 7, No. 6, Nov.–Dec. 1991, pp. 922–928. doi:10.2514/3.23410
[26] Rosenberg, S. D., Gage, M. L., Homer, G. D., and Franklin, J. E., "Hydrocarbon-Fuel/Copper Combustion Chamber Liner Compatibility, Corrosion Prevention, and Refurbishment," *Journal of Propulsion and Power*, Vol. 8, No. 6, Nov.–Dec. 1992, pp. 1200–1207. doi:10.2514/3.11462
[27] Brown, S. P., and Frederick, R. A., "Laboratory-Scale Thermal Stability Experiments on RP-1 and RP-2," *Journal of Propulsion and Power*, Vol. 24, No. 2, 2008, pp. 206–212. doi:10.2514/1.27724
[28] Wagner, W. R., and Shoji, J. M., "Advanced Regenerative Cooling Techniques for Future Space Transportation Systems," 11th AIAA/SAE Propulsion Conference, Anaheim, CA, AIAA No. 75-1247, 1975.
[29] Cook, R. T., and Quentmeyer, R. J., "Advanced Cooling Techniques for High Pressure Hydrocarbon-Fueled Rocket Engines," 16th AIAA/SAE/ASME Joint Propulsion Conference, Hartford, CT, AIAA Paper 80-1266, 1980.
[30] Irvine, S. A., Schoettmer, A. K., Bates, R. W., and Meyer, M. L., "History of Sulfur Content Effects on the Thermal Stability of RP-1 Under Heated Conditions," 40th AIAA/ASME/SAE/ASEE Joint Propulsion Conference and Exhibit, Fort Lauderdale, FL, July 2004, AIAA Paper 2004-3879.
[31] Stiegemeier, B., Meyer, M. L., and Taghavi, R., "A Thermal Stability and Heat Transfer Investigation of Five Hydrocarbon Fuels: JP-7, JP-8, JP $-$ 8 $+$ 100, JP-10, and RP-1," 38th AIAA/ASME/SAE/ASEE Joint Propulsion Conference and Exhibit, Indianapolis, IN, AIAA Paper 2002-3873, July 2002.
[32] Coguill, S. L., "Synthesis of Highly Loaded Gelled Propellants," Resodyn Corp., Butte, MT, 2009.
[33] Braun, D. B., and Rosen, M. R., *Rheology Modifiers Handbook: Practical Use and Application*, William Andrew, Norwich, NY, 2000.
[34] Cedeño, F. O., Prieto, M. M., Espina, A., and García, J. R., "Fast Method for the Experimental Determination of Vaporization Enthalpy by Differential Scanning Calorimetry," *Journal of Thermal Analysis and Calorimetry*, Vol. 73, 2003, pp. 775–781. doi:10.1023/A:1025878313429
[35] Arnold, R., Santos, P. H. S., Kubal, T., Campanella, O., and Anderson, W. A., "Investigation of Gelled JP-8 and RP-1 Fuels," *Proceedings of the World Congress on Engineering and Computer Science 2009*, Vol 1, San Francisco, Oct. 2009, pp. 63–68.
[36] Outcalt, S., Laesecke, A., and Brumback, K. J., "Thermophysical Properties Measurements of Rocket Propellants RP-1 and RP-2," *Journal of Propulsion and Power*, Vol. 25, No. 5, Sept.–Oct. 2009, pp. 1032–1040. doi:10.2514/1.40543
[37] Ueno, K., Hata, K., Katakabe, T., Kondoh, M., and Watanabe, M., "Nanocomposite Ion Gels Based on Silica Nanoparticles and an Ionic Liquid: Ionic Transport, Viscoelastic Properties, and Microstructure," *Journal of Physical Chemistry B*, Vol. 112, No. 30, 2008, pp. 9013–9019. doi:10.1021/jp8029117
[38] Yokoyama, K., Koike, Y., Masuda, A., and Kawaguchi, M., "Rheological Properties of Fumed Silica Suspensions in the Presence of Potassium Chloride," *Japanese Journal of Applied Physics*, Vol. 46, No. 1, 2007, pp. 328–332. doi:10.1143/JJAP.46.328
[39] Turns, S. R., *An Introduction to Combustion-Concepts and Applications*, Series in Mechanical Engineering, 2nd ed., McGraw–Hill, New York, 2000.
[40] Glassman, I., *Combustion*, 3rd ed., Academic Press, San Diego, CA, 1996.
[41] Nachmoni, G., and Natan, B., "Combustion Characteristics of Gel Fuels," *Combustion Science and Technology*, Vol. 156, 2000, pp. 139–157. doi:10.1080/00102200008947300
[42] Mita, I., Imai, I., and Kambe, H., "Determination of Heat of Mixing and Heat of Vaporization with a Differential Scanning Calorimeter," *Thermochimica Acta*, Vol. 2, 1971, pp. 337–344. doi:10.1016/0040-6031(71)85035-9
[43] Jones, D. E. G., Feng, H. T., Augsten, R. A., and Fouchard, R. C., "Thermal Analysis Studies on Isopropylnitrate," *Journal of Thermal Analysis and Calorimetry*, Vol. 55, 1999, pp. 9–19. doi:10.1023/A:1010190829563
[44] Rapp, D. C., and Zurawski, R. L., "Characterization of Aluminium/RP-1 Gel Propellant Properties," 24th AIAA/ASME/SAE/ASEE Joint Propulsion Conference, Boston, AIAA Paper 88-2821, July 1988.

L. Maurice
Associate Editor